



Ageing of dental zirconia ceramics

Tomaž Kosmač^{a,b,*}, Andraž Kocjan^a

^a Engineering Ceramics Department, Jožef Stefan Institute, SI-1000 Ljubljana, Slovenia

^b Centre of Excellence NAMASTE, SI-1000 Ljubljana, Slovenia

Abstract

An *in vitro* study was designed to monitor the t–m transformation of biomedical grade 3Y-TZP ceramics produced from two ready-to-press granulated powders of the same nominal chemical composition, but differing in their specific surface area. Disc-shaped specimens were formed by uni-axial dry-pressing and sintering in air for 2 h in the temperature range 1400–1550 °C, resulting in a mean grain size of 0.26–0.57 μm. The sintered specimens were subjected to accelerated ageing in deionized water at 134 °C for up to 48 h and verified in terms of the amount of the transformed monoclinic fraction, the thickness of the transformed layer, and the bi-axial flexural strength. The sintering-temperature-dependent transformability during ageing was confirmed, whereby the role of the starting-powder characteristics was more pronounced at lower sintering temperatures and was almost negligible at higher sintering temperatures.

© 2012 Elsevier Ltd. All rights reserved.

Keywords: ZrO₂ (Y-TZP); Biomedical (dental) applications; Corrosion (ageing)

1. Introduction

Yttria partially stabilized tetragonal zirconia (Y-TZP) holds a unique place among dental ceramics because of its excellent tissue compatibility and superior strength, fracture toughness and damage tolerance, compared to other dental ceramics.^{1–3} These capabilities are very attractive in prosthetic dentistry, where esthetics and strength are paramount. The superior mechanical properties of Y-TZP ceramics, compared to other bioceramics^{4–6} allow them to be used for the fabrication of multi-unit posterior bridges. Additionally, they enable a substantial thickness reduction of those fixed partial dentures (FPDs) in the visible part of the dental arch that are subjected to lower mechanical stresses.⁷ However, the main driving force for the replacement of traditional metal-based FPDs with all-ceramic prosthetic crowns and bridges is the improved esthetics and excellent tissue compatibility achieved using tooth-colored, metal-free systems. In the beginning, ceramic frameworks were produced by the extremely expensive and time-consuming process of the precise hard-milling of densely sintered and hot isostatically pressed (HIP) Y-TZP zirconia blocks, followed by veneering. However,

since its development in 2001, the direct oversize milling of biscuit-sintered Y-TZP blanks has become increasingly popular in dentistry and is now the most common method for the fabrication of individual Y-TZP cores for all-ceramic dental restorations.⁸ In this manufacturing technology, the die or a wax pattern is scanned, and an enlarged restoration is designed by computer software (CAD) and a pre-sintered ceramic blank is oversize-milled using computer-aided machining. The restoration is then pressure-less sintered to near-theoretical density. The last processing step before the final adjustment and cementation is porcelain veneering, aimed at achieving the required shape and shade. Although the starting-powder source and the type of blank-pressing procedures applied by each manufacturer are proprietary information, it is no secret that the vast majority of commercially available zirconia blanks are made of a raw material from the same Japanese powder manufacturer Tosoh (Tokyo, Japan), which offers two ready-to-press, water-resistant, bio-medical powder grades of the same chemical composition but differing in their specific surface area and thereby related pressing and sintering ability. Zirconia blanks are commonly performed by uniaxial dry pressing in a floating die at a low pressure, followed by cold isostatic pressing (CIP) and biscuit sintering. Typical pre-sintering temperatures for the high- and low-specific-area powder grades are 1000 °C and 1100 °C, respectively. The recommended sintering temperatures for soft-milled FPDs from the high- and low-specific-area powder grades range from 1350 °C to 1450 °C and from 1450 °C to 1550 °C,

* Corresponding author at: Engineering Ceramics Department, Jožef Stefan Institute, SI-1000 Ljubljana, Slovenia. Tel.: +386 14773227; fax: +386 14773171.

E-mail address: tomaz.kosmac@ijs.si (T. Kosmač).

respectively. Hence, depending on the starting-powder grade and the sintering conditions, a variety of sintered Y-TZP ceramics can be fabricated, exhibiting different grain size, phase composition, transformability and mechanical properties.

Under clinical conditions, all-ceramic dental restorations are exposed to a state of biaxial stress with the interior (cementation) surface loaded in tension.⁹ Critical loads for the initiation of catastrophic failure tend to diminish steadily with time, from stress corrosion and fatigue as well as from secondary degradation mechanisms, such as cracks introduced during air-particle abrasion and/or enhanced ageing pertaining to Y-TZP ceramics.¹⁰ When exposed to an aqueous environment at slightly elevated temperatures over long periods, the surface of the Y-TZP ceramic will start transforming spontaneously into the monoclinic structure *via* a stress-corrosion-type mechanism.^{11,12} The process is accompanied by extensive micro-cracking, which ultimately leads to strength degradation.¹² Thus, in 2001–2002, several hundreds of Y-TZP femoral heads failed in a short period, with the origin of the fracture clearly associated with hydrothermal degradation. Based on the results obtained with retrieved zirconia femoral heads the ageing behavior of orthopedic zirconia *in vivo* is well documented and can be predicted using an *in vitro* accelerated-ageing test,¹³ but in spite of the lesson learned from orthopedics, no such systematic ageing study with dental ceramics under clinical conditions has been performed so far. Until recently, dentists were not concerned with ageing problems, presumably anticipating that veneering porcelain and luting materials, separating the core from the oral environment, and hard dental tissues provide a durable protection of the dental zirconia against hydrothermal decomposition.

However, some parts of the FPD may not be entirely covered with porcelain, and it has been shown recently that commonly used luting cements absorb water *via* dentine tubules, thereby exposing the interior core surface to moisture, which, in turn, may lead to severe ageing problems over a considerably shorter period of time than anticipated.¹⁴

Here we report on the results of an *in vitro* study designed to monitor the propagation of the t–m transformation of 3Y-TZP ceramics produced from the two most commonly used ready-to-press granulated powders for dental applications that were sintered at different temperatures to produce sintered materials differing in their grain size, phase composition, transformability and mechanical properties. Since there is a strong grain-size dependence of the transformability of Y-TZP ceramics, it is likely that the choice of the starting powder and sintering conditions will play an important role in *in vitro* accelerated ageing behavior during the hydrothermal surface treatment and thereby the related reliability of sintered dental zirconia.

2. Experimental

2.1. Specimen preparation and characterization

Two commercially available, ready-to-press, granulated, biomedical-grade, Y-TZP powders (Tosoh, Japan) were used for the preparation of specimens: a low-calcined TZ-3YB-E grade

with a higher specific surface area ($7 \text{ m}^2/\text{g}$) and a high-calcined TZ-3YSB-E grade with a lower specific surface area ($16 \text{ m}^2/\text{g}$). Both powders were of the same nominal chemical composition, containing 3 mol% yttria in the solid solution to stabilize the tetragonal structure, 0.25 wt% of alumina to suppress ageing, *i.e.*, the t–m transformation during ageing in an aqueous environment, and 3 wt% of an acrylic binder. Uni-axial dry pressing at 150 MPa in a floating die was used to shape green disks of 20 mm in diameter and 2 mm in thickness, which were subsequently pressure-less sintered in air for 2 h in the temperature range 1400–1550 °C. The sintering temperature was incrementally increased in 50 °C intervals. After sintering, the ceramic specimens were verified for fractional density and mean grain size, and subjected to accelerated ageing at 134 °C in deionized water. The densification behavior of both granulated Y-TZP powders was followed with a dilatometric analysis in which dry-pressed (at 150 MPa) samples in the form of pellets ($\Phi = 6 \text{ mm}$, $h = 6 \text{ mm}$) were heated to 1550 °C at a heating rate of 10 °C/min. Once the final temperature was reached, samples were cooled down without any dwell, the cooling rate being 10 °C/min up to 400 °C, and then the furnace was switched off.

The fractional density of the green compacts was evaluated geometrically, while the fractional density of the sintered disks was determined with Archimedes' method using distilled water as the immersion liquid. Even though the specimens were sintered in the two-phase (t+c) region, the relative densities were calculated by adopting a theoretical density of $\rho_T = 6.08 \text{ g/cm}^3$ for the tetragonal phase. The grain size evaluations were made on FE-SEM (Carl Zeiss, Supra 35LV, Oberkochen, Germany) micrographs of polished ($3 \mu\text{m}$ diamond paste) and thermally etched (1380 °C, 1 h) specimens, using the linear interception method, based on the ASTM E112-96(2004)e2 standard. Dilatometric measurements were performed to follow the densification behavior. The heating rate was 10 °C/min. X-ray diffraction patterns in the $25\text{--}40^\circ 2\theta$ range were collected from the specimen's surfaces before and after accelerated ageing experiments using

Cu K α radiation (PANalytical X'Pert PRO diffractometer). The presence of tetragonal, monoclinic and cubic zirconia was confirmed according to the JCPDS data (File card Nos. 80-2187, 80-2187 and 80-2187, respectively).

The relative amount of the transformed monoclinic zirconia (m-ZrO₂) on all the surfaces was determined from the integral intensities of the monoclinic ($\bar{1}11$)_m and (111)_m, and the tetragonal (101)_t peaks according to the method of Garvie and Nicholson, which is the most commonly applied to determine the phase composition of zirconia powders and compacts with randomly distributed m-ZrO₂ and t-ZrO₂ phases at any distance from the surface exposed to the XRD analysis.¹⁵

2.2. *In vitro* ageing

No surface treatment, such as grinding and/or polishing was applied to specimens' surface before *in vitro* ageing experiments. These were conducted in distilled water under isothermal conditions at 134 °C for 6–48 h. Even though the ceramic FDPs are not sterilized, use of water stream and the sterilization

temperature were adopted from the new ISO standard for surgical Y-TZP implants, the ISO 13356 standard recommendations for zirconia Y-TZP-based implants for surgery. After autoclaving, the specimens were analyzed using the X-ray diffraction (XRD) technique for the phase composition, as recommended by the ISO 13356 standard. In addition, the thickness of the transformed monoclinic fraction ($m\text{-ZrO}_2$) after autoclaving was measured from SEM images on gently ground cross-sections. For this, the specimens were cut with a diamond blade and the cross-sections were ground using SiC grinding paper (240 grit). The measured values were compared to the estimated transformation depth, as calculated using the XRD method originally developed by Kosmač et al.¹⁶ back in 1982 for ceramics containing tetragonal ZrO_2 . According to this method, the transformation zone depth a can be expressed by:

$$a = \frac{(\ln((X_{\text{bulk}} - X_{\text{trans}})/(X_{\text{meas}} - X_{\text{trans}}))}{2\mu} \sin \theta \quad (1)$$

where X_{bulk} stands for the monoclinic zirconia fraction in the bulk of the starting material (*i.e.* at a distance $x > a$ below the surface), X_{trans} is the estimated maximum fraction of the tetragonal ZrO_2 that can be transformed to monoclinic ZrO_2 within the transformation zone, *i.e.* at a distance $0 < x < a$, and X_{meas} is the monoclinic zirconia fraction, obtained from XRD data as measured on the surface of the mechanically (grinding, sandblasting, fracture) or hydrothermally (ageing in an aqueous environment) treated ceramic, θ is the angle of reflection of the incident beam, and μ the absorption coefficient. In the case of 3Y-TZP ceramics subjected to accelerated ageing, no monoclinic phase was detected on the surface of as sintered ceramics ($X_{\text{bulk}} = 0$); from the Scott's phase diagram estimated amount of the cubic zirconia phase that won't transform to monoclinic upon ageing ranged from 24% (at 1400 °C) to 29% (at 1550 °C), whereas the remaining tetragonal can be consider as transformable to monoclinic ($0.71 < X_{\text{trans}} < 0.76$), for Cu K α irradiation, $\theta = 15^\circ$ and $\mu = 0.0642$ for the Y_2O_3 -stabilized tetragonal ZrO_2 (3Y-TZP).¹⁷

Preliminary biaxial, flexural strength measurements were performed according to ISO 6872 at a loading rate of 1 mm/min, using a universal testing machine (Model 4301, Instron Corp., Canton, USA). The tests were performed only on specimens that were aged for 24 h. Four specimens from each group were tested in deionized water; the average and the corresponding SD were calculated, but no attempt was made to further elaborate the results and/or analyze the fracture surfaces.

3. Results and discussion

3.1. Sintering behavior

The dilatometric curves and the temperature-dependent densification rate of the dry-pressed TZ-3YB-E and TZ-3YSB-E powder compacts are shown in Fig. 1. The corresponding relative density of the green test bodies was 47.2% and 49.5%, respectively. In agreement with the powder manufacturer's specifications, the finer TZ-3YB-E material exhibiting the higher specific surface area starts to shrink at approximately 900 °C, which is an about 100 °C lower temperature compared to the

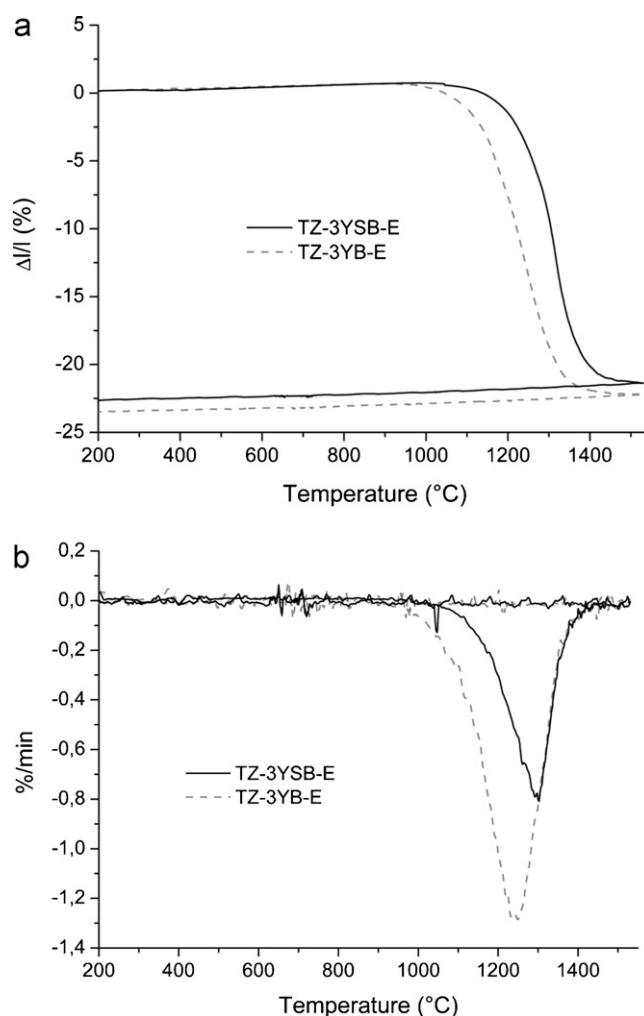


Fig. 1. Dilatometric curves of granulated biomedical-grade TZ-3YB-E and TZ-3YSB-E powders, which were uni-axially dry pressed at 150 MPa in a floating die and heated to 1550 °C, with 10 °C/min heating rate and no dwell time: (a) linear shrinkage versus temperature and (b) densification rate versus temperature.

lower-specific-surface-area TZ-3YSB-E material. During the initial stage of sintering, the low-calcined, high-BET powder compact shrinks faster than the high-calcined, low-BET material, and there is a marked difference between the two powder compacts for the temperature at which the maximum densification rate is reached. However, at 1350 °C, the shrinkage rate of both materials became almost identical and remained identical until the final temperature was reached (Fig. 1b). These results tend to indicate that the starting powder characteristics (in particular BET) strongly influence the initial stages of sintering, during which the surface diffusion is prevailing, whereas during the last stage of sintering, which is dominated by the volume diffusion and grain-boundary mobility, the effect of the starting powder's characteristics becomes almost negligible. With reference to Fig. 1a, there was a marked (1–2%) difference in the sintering shrinkage between the two powder compacts. However, since these samples differ in terms of the green density, no conclusion can be made regarding the final density of the sintered ceramics.

Table 1

The temperature-dependent fractional theoretical density (TD) of the sintered TZ-3YB-E and TZ-3YSB-E disks determined by the Archimedes method using distilled water as immersion liquid.

Temperature (°C)		1400	1450	1500	1550
TD (%)	TZ-3YB-E	99	99	99.1	99.1
	TZ-3YSB-E	98.5	99	99.2	99.2

3.2. Density and microstructure

The relative densities of sintered TZ-3YB-E and TZ-3YSB-E disks are listed in Table 1 in which the information on the estimated accuracy of the measuring method and variability in density, *e.g.* standard deviation, was intentionally skipped. As indicated in Section 2, sintering of a zirconia powder compact containing 3 mol% of yttria in a two phase region will yield ceramic consisting of tetragonal zirconia ($t\text{-ZrO}_2$) with less than 3 mol% of yttria in the solid solution, and cubic zirconia ($c\text{-ZrO}_2$) with $\gg 3$ mol% of yttria in the solid solution. According to Ruiz et al.,¹⁸ there is a lot of uncertainties associated with the determination of the relative amount of the cubic zirconia in sintered Y-TZP when using quantitative XRD analysis. This is due to the large similarity of the t and c unit cells resulting in overlap of most high intensity reflections in the XRD pattern. For this reason Ruiz et al.¹⁸ suggested using a theoretical calculation of the t/c ratio from an equilibrium phase diagram instead. They used the phase diagram by Scott,¹⁹ and ignored the temperature-dependent variation in the amount of yttria in the t and c solid solutions, *i.e.* they used constant theoretical density values for the t and c phase regardless on the sintering temperature, which seems to be a common practice in papers dealing with sintered Y-TZP ceramics. The benefit of doing so is that the results obtained in that way are comparable to other reports, a drawback being that the calculated relative density values represent (over)estimates with a sintering temperature-dependent deviation from the true value.

Anyway, while at 1400 °C the TZ-3YB-E ceramic is already almost fully dense, *i.e.* exhibiting 99.5% of the TD, the TZ-3YSB-E material reaches the same relative density at an about 50 °C higher sintering temperature, which is in agreement with the dilatometric analysis (Fig. 1).

SEM micrographs obtained from the sintered and thermally etched surfaces of the TZ-3YB-E and TZ-3YSB-E ceramics shown in Fig. 2(a–d) are aimed at illustrating (i) the sintering temperature dependent grain size and, more importantly, (ii) almost identical grain size of the two ceramic grades when sintered under the same conditions. As expected, increasing the sintering temperature resulted in coarser microstructures of the specimens. Notice, that irrespective of the difference in the specific surface area of the starting TZ-3YB-E and TZ-3YSB-E powders, the ceramic microstructures after sintering under the same conditions are practically identical, being uni-modal, exhibiting similar grain sizes and with no pore inclusions. Some alumina grain inclusions (darker grains) were also detected (Fig. 2b and c).

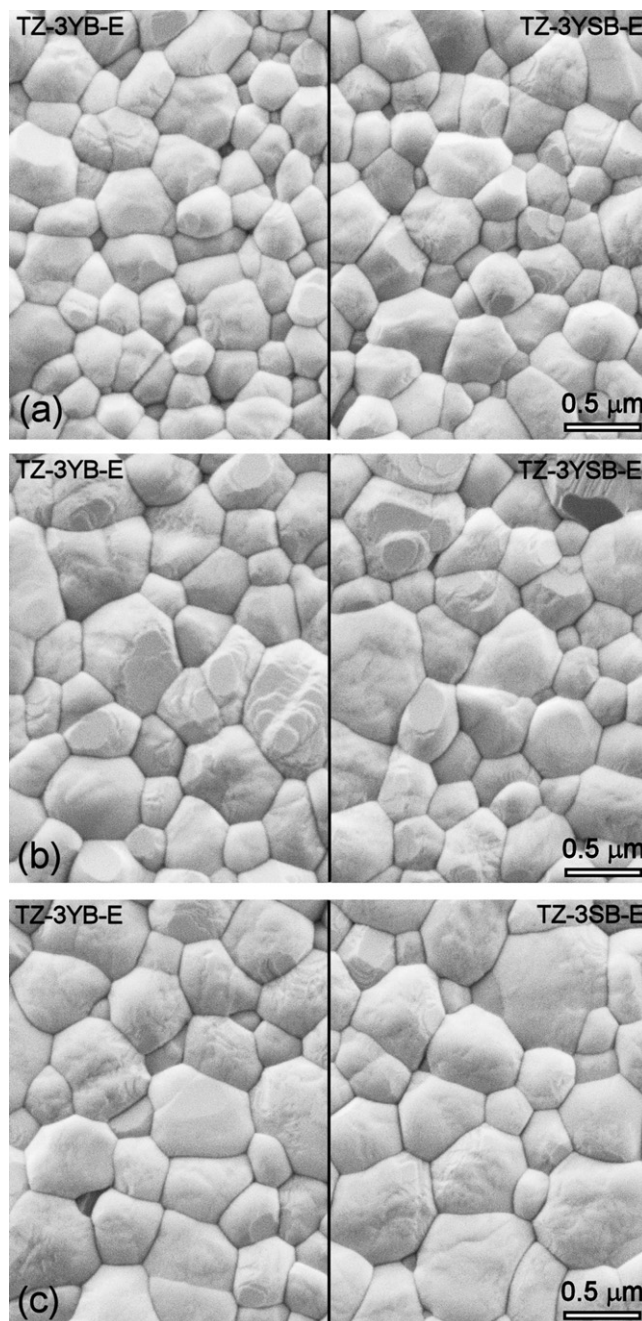


Fig. 2. SEM micrographs of polished and thermally etched surfaces of the TZ-3YB-E and TZ-3YSB-E ceramics sintered for 2 h at (a) 1400 °C, (b) 1450 °C, (c) 1500 °C and (d) 1550 °C.

The variation in grain size of the two materials with the sintering temperature that is graphically represented in Fig. 3 indeed shows an almost complete overlapping of the two curves in the investigated temperature region (1400–1550 °C), in agreement with the results of dilatometric analysis (Fig. 1). Also with reference to results of the dilatometric analysis in Fig. 1, the remarkable similarity in the resultant microstructure further indicates an almost identical grain growth kinetics in the both materials during the final stage of sintering.

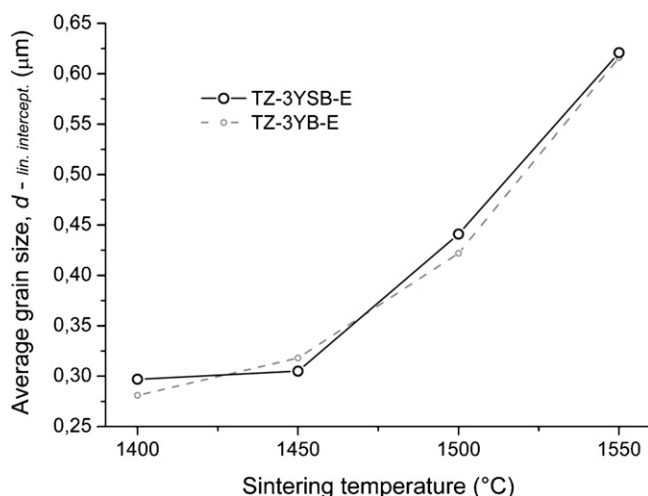


Fig. 3. Sintering-temperature-dependent average grain sizes of TZ-3YB-E and TZ-3YSB-E ceramics evaluated by using the linear interception method.

3.3. Phase composition

Fig. 4 shows typical X-ray diffraction patterns in the 25–40 2θ range obtained from the surface of TZ-3YSB-E ceramics, sintered for 2 h at 1400 °C and 1550 °C. The pattern of the low-temperature (1400 °C) sintered ceramic displays three characteristic peaks positioned at 2θ of 30.2°, 34.7° and 35.2° corresponding to the (1 0 1)_t, (0 0 2)_t and (1 1 0)_t planes of the t-ZrO₂ phase, respectively. Sintering of the same powder grade at higher temperature of 1550 °C resulted in the appearance of an additional reflection at 35° 2θ (inset Fig. 4) characteristic for the c-ZrO₂ (2 0 0)_c plane. The increased intensity of the diffraction peak positioned at 30.2° 2θ in this pattern can be therefore attributed to the emergence of the (1 1 1)_c plane reflection overlapping with the (1 0 1)_t reflection. As already mentioned, the fraction of c-ZrO₂ was not quantified using XRD analysis; instead, for any sintering temperature the equilibrium volume

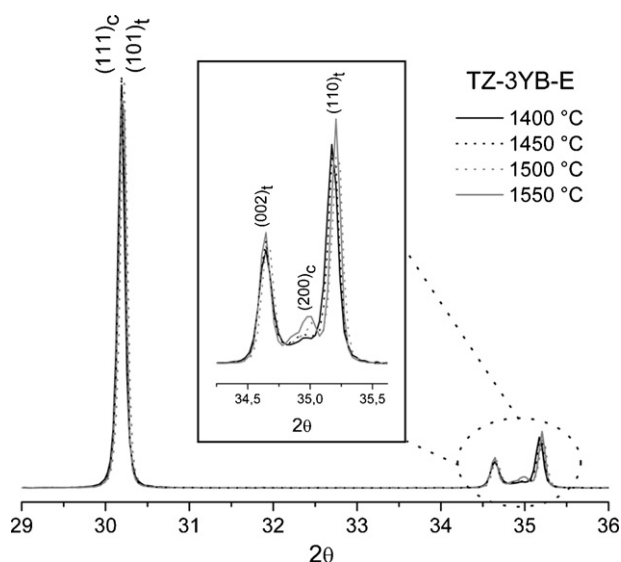


Fig. 4. Comparison of XRD patterns obtained from TZ-3YB-E ceramic surfaces, sintered for 2 h at 1400 °C and 1550 °C.

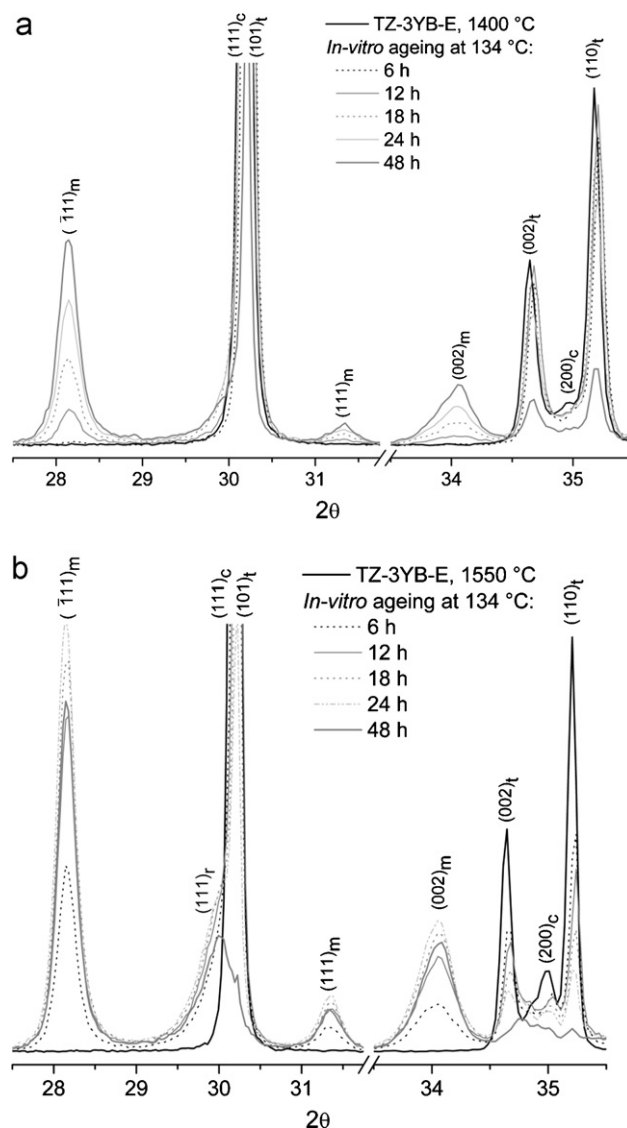


Fig. 5. XRD patterns obtained from TZ-3YB-E ceramic surfaces, sintered for 2 h at a) 1400 °C and b) 1550 °C, which were additionally aged in water at 134 °C for 6, 12, 18, 24 and 48 h.

fraction and was estimated using the lever rule on the Scott's ZrO₂–Y₂O₃ equilibrium phase diagram.¹⁹ The amount of the m-ZrO₂ in all the sintered specimens was below the detection limit. The same holds for the rhombohedral (cubic 2; r-ZrO₂) phase.

3.4. Accelerated in vitro aging behavior

Characteristic XRD patterns obtained from TZ-3YB-E ceramic surfaces sintered for 2 h at the lowest (1400 °C) and the highest (1550 °C) temperature, before and after accelerated ageing at 134 °C in water for different periods of time (6, 12, 18, 24 and 48 h), are represented in Fig. 5a and b, respectively. Notice that the intensity of the (2 0 0)_c peak (at 2θ = 35°) of the reference material (*i.e.* ceramic before accelerated ageing) that was sintered at higher temperature is considerably higher, compared to that obtained from the reference material sintered at lower

temperature also confirming a higher amount of the c-ZrO₂ phase in the former material. Accelerated ageing for a short period of time (6 h) has not resulted in any marked difference in the XRD pattern obtained from the surface of the two materials implying only minor (negligible) changes in the phase composition on the surfaces. After 12 h of ageing, however, monoclinic ($\bar{1}11$)_m, (111)_m, and (002)_m peaks (positioned at 2θ of 28.15°, 31.3°, and 34°, respectively) start emerging with a tendency for their intensity to increase with still longer ageing times at the expense of reduced intensity of the tetragonal (101)_t, (002)_t and (110)_t peaks. Also worth mentioning here is that, with prolonged ageing time, not only the intensity of t-ZrO₂ peaks but also that of the (200)_c peak is decreasing, accompanied by markedly asymmetric (111)_c/(101)_t peak broadening, presumably due to the emergence of the (111)_r peak.^{20–22} The latter could be attributed to the lattice distortion of the t/c-ZrO₂ resulting in the formation of a r-ZrO₂ phase, commonly observed with ground, abraded/cut or fractured surfaces accompanied by a reversed intensity of the (002)_t and (110)_t peaks in the XRD pattern. The formation of r-ZrO₂ has also been reported with ion-implanted surfaces of both partially (3 mol% Y₂O₃), and fully (8 mol% Y₂O₃) stabilized zirconia,²³ whereas in aged Y-TZP ceramics the additional peak at $2\theta = 29.8^\circ$ contributing to the asymmetric (101)_t peak broadening is usually denoted as (ascribed to the presence of) the (111)_c peak, or it is simply ignored. However, as demonstrated by Kim et al.,²⁴ ageing of Y-TZP is not only capable of inducing the t–m transformation but also the t–r phase transformation. According to these authors, the latter is most probably due to compressive stresses exerted on t-ZrO₂, as a result of the volume expansion associated with the t–m transformation. In the very same work, an increasing r-ZrO₂ fraction with increasing amount of the transformed monoclinic zirconia has been demonstrated, but no attention was paid to the intensity of the (002)_t and (110)_t peaks. Anyway, with reference to Fig. 5, the asymmetric (101)_t/(111)_c peak broadening in our samples is more pronounced in the ceramic sintered at the higher temperature (Fig. 5b) indicating a higher amount of the r-ZrO₂ in this material. In fact, after 48 h of accelerated ageing of this material, the intensity of the (111)_r phase becomes stronger than the intensity of the tetragonal (101)_t peak, but no significant change in the intensity of the (002)_t/(110)_t peak ratio could (can) be observed. Without knowing the origin and evolution of the r-ZrO₂ phase on the surface of *in vitro* aged Y-TZP ceramics, any explanation for the preserved intensity of (002)_t and (110)_t peaks in *in vitro* aged Y-TZP ceramics would be premature and the same holds for the observed sintering temperature-dependent amount of the distorted high-temperature zirconia phase.

In spite of ambiguities associated with the phase composition of the surface layer after ageing, the relative amount of transformed monoclinic zirconia was calculated, whereby the integral intensity of the asymmetric peak spreading from $2\theta = 29.3$ – 30.5° was considered as the untransformed fraction. The results showing the variation of the calculated fraction of the monoclinic zirconia for the two starting powders and all sintering temperatures with *in vitro* ageing time is represented in Fig. 6.

Materials sintered at higher temperatures initially transform at a higher rate than those sintered at lower temperatures. Also,

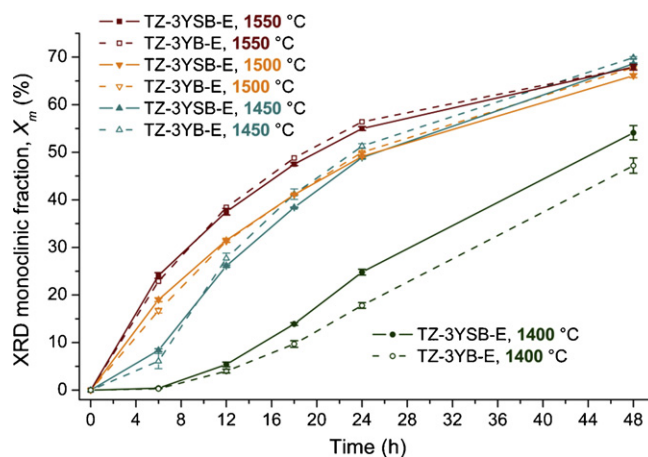


Fig. 6. Calculated fraction of monoclinic zirconia (X_m) versus accelerated *in vitro* ageing time for the TZ-3YSB-E and TZ-3YB-E ceramic surfaces, sintered for 2 h in the temperature range 1400–1550 °C.

there was a marked difference in ageing behavior between the two materials sintered at the lowest sintering temperature of 1400 °C, in spite of the fact that at any sintering temperature the grain size achieved with the two powder grades differing in the specific surface area was almost identical (see Fig. 3). This observation warrants attention as it implies that in this particular case the grain size was not the prevailing factor influencing the transformability of t-ZrO₂ under hydrothermal conditions. Since for higher sintering temperatures there was no significant difference in the ageing behavior between the two starting powders, the observed difference in ageing behavior between materials sintered at the lowest temperature could be either due to a slight difference in the phase composition, or due to a slight difference remnant intergranular porosity and thereby related internal stresses developed in the grain boundaries,²⁵ but no attempt was made so far to experimentally confirm any of these speculations. Anyhow, with prolonged ageing time of materials sintered at temperatures higher than 1400 °C the difference in the amount of transformed monoclinic fraction was getting ever smaller, until after 48 h of accelerated ageing the amount of transformed monoclinic zirconia on the surface of these materials became nearly the same. With still longer ageing time, the X_m value as determined on the specimens' surfaces using XRD reached the so-called saturation indicating that the thickness of the transformed layer equalled or exceeded the penetration depth of the incident Cu K α irradiation.

Here again, no answer can be given at this point what were the remaining phases coexisting with the monoclinic zirconia in the transformed surface layer, once the saturation is reached, and how they are related to the particular material processing variables and ageing conditions.

In order to get additional information related to ageing behavior of tested materials, the XRD data collected from the aged specimens' surfaces were inserted into Eq. 1 to calculate the thickness of the transformed surface layer upon accelerated *in vitro* ageing. The results are graphically presented in Fig. 7. As already mentioned in Section 1, the XRD method anticipates homogeneous distribution of detected phases in the analyzed

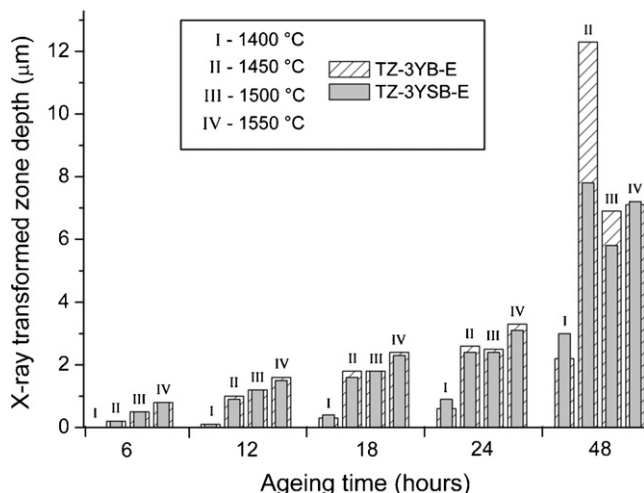


Fig. 7. Transformed zone depth of the monoclinic fraction layer for the TZ-3YB-E and TZ-3YSB-E ceramics versus sintering temperature and accelerated *in vitro* ageing time evaluated from the X-ray data.

volume and is not applicable to specimens exhibiting heterogeneous phase distribution on, or close below the surface. Yet another practical limitation of the method arises from the exponential drop of the reflected integral intensity with the distance from the analyzed surface. Once the thickness of the transformed layer becomes equal to, or exceeds the penetration depth of the incident irradiation, the XRD determination method becomes insensitive to any changes in the composition that may occur deeper in the bulk. In spite of these limitations and previously mentioned uncertainties associated with the exact phase composition of the as-sintered ceramics, the XRD determination method at least gave us an idea about the thickness of the transformed layer in relation to the processing variables, *e.g.* the sintering temperature, microstructural characteristics and *in vitro* ageing conditions. If, for example, the estimated transformed zone depth is equal or smaller than the average grain size, it can be assumed that only part of surface grains has been transformed upon ageing, such as in the case of the low-temperature sintered ceramics during the initial 12 h of ageing. In the case of high-temperature sintered ceramics, in contrast, a continuous, about 1–2 grains thick surface layer can already be expected under the same ageing conditions. After prolonged ageing of 48 h, the transformed layer is likely to be extended over about twenty grains from the surface into the bulk of the very same material.

Characteristic SEM micrographs of polished and thermally etched specimens that were subjected to an accelerated *in vitro* ageing in water at 134 °C for various periods of time are presented in Fig. 8. In contrast to smooth as-sintered surfaces (shown in Fig. 2), several self-accommodating martensitic variants (laths) of various orientations are visible on the specimen's surface after ageing that either intersect within a single grain, or they grow continuously from grain to grain, as already reported elsewhere.²⁶ Notice that the number of martensitic laths in the surface of specimens aged for 6 h (Fig. 8a) is considerably lower than that in the surface of specimens aged for 24 h (Fig. 8b), while the surface topography of specimens aged for 24 h and 48 h

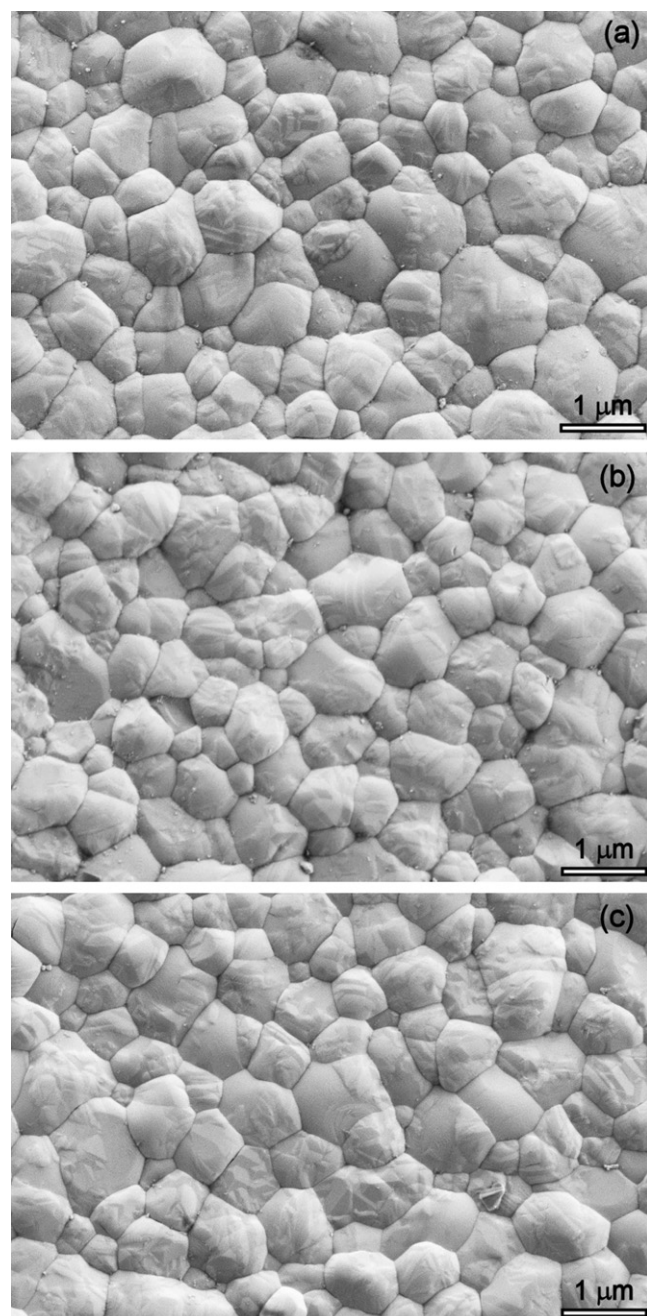


Fig. 8. SEM micrographs of polished and thermally etched surfaces of TZ-3YSB-E ceramics sintered at 1550 °C for 2 h and after additional accelerated *in vitro* ageing in water at 134 °C for (a) 6 h, (b) 24 h and (c) 48 h.

(Fig. 8c) is very much alike implying a similar surface density of the martensitic laths in these two specimens that differed in the duration of *in vitro* ageing for a factor of two. These observations are in line with findings of Deville and Chevalier,²⁶ who used AFM in the observation of the initial stages of martensite relief growth in Y-TZP ceramics. According to these authors, ageing of Y-TZP ceramics involves spontaneous transformation of the tetragonal grains into the monoclinic structure by a nucleation and growth process, which initiates from isolated surface grains, and gradually proceeds into the bulk *via* a stress-corrosion-type mechanism. In order to further support this assumption,

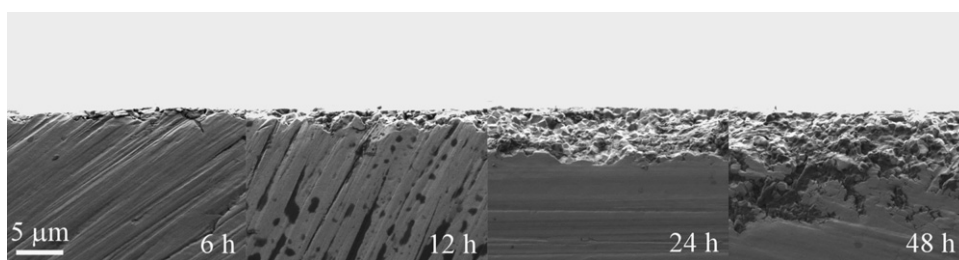


Fig. 9. SEM micrograph of the diagonally cut and ground surfaces of the TZ-3YSB-E ceramics sintered at 1550 °C for 2 h and after accelerated *in vitro* ageing in water at 134 °C for 6, 12, 24 and 48 h.

Table 2

Transformed zone depth of the monoclinic fraction layer for the TZ-3YSB-E and TZ-3YB-E ceramics *versus* sintering temperature and accelerated *in vitro* ageing time evaluated from SEM micrographs.

SEM [μm]				
134 °C	24 h		48 h	
T (°C)	B-E	SB-E	B-E	SB-E
1400	Not measured	3.1	3.7	
1450	2.4	1.9	4.7	5.4
1500	2.6	2.3	7.1	6.2
1550	3.5	3.2	8.2	7.5

specimens aged for different periods of time were cut and gently ground to obtain cross-sections for subsequent SEM analysis. They were aimed at estimating the thickness of the transformed layer, by anticipating that under gentle grinding the wear of the transformed surface layer will differ from that of the tetragonal bulk²⁷. As illustrated in Fig. 9, after the initial 6 h of *in vitro* ageing applied to the particular material chosen to exemplify typical microstructural features obtained from ground cross-sections, only a few sporadic pullouts are visible on the specimen's surface, whereas after 12 h of ageing, a thin but continuous layer with crumbled appearance is already clearly distinguished from the bulk; after still longer ageing times the thickness of this layer became large enough to be measured. One has to be aware, however, that due to extremely uneven line separating the surface layer from the bulk of gently ground cross-sections, a relatively large scatter in the measured values should be encountered. Nevertheless, the distance of the sharp uneven line from the surface of sintered Y-TZP ceramics after 24 h and 48 h of ageing was determined and the results are listed in Table 2. Notice that no continuous surface layer could be observed on the ground cross-sections of the two materials sintered at the lowest sintering temperature after ageing for 24 h. This observation is in line with the results obtained by XRD analysis revealing that these two materials transform at a lower rate compared to materials sintered at higher temperatures. Also, materials sintered at higher temperatures transform deeper than those sintered at lower temperatures and there is a strong ageing time dependence of the transformed zone depth. It is worth mentioning, however, that even after prolonged ageing the difference between the investigated sintering temperatures is preserved, in contrast to results of XRD analysis in Fig. 6 showing nearly the same amount of transformed monoclinic zirconia after 48 h of

ageing in all tested materials that were sintered above 1400 °C. The SEM method clearly has a potential of demonstrating the difference between materials sintered at different temperatures after prolonged ageing, but the method does not allow making conclusion regarding the difference in ageing behavior between ceramics fabricated from the two starting powder grades of the same chemical composition but differing in their specific surface area.

It is worth mentioning here that in spite of several uncertainties and inherent limitations pertaining to the two determination methods used in the work, the agreement of results presented in Fig. 7 and Table 2 is quite remarkable. It should be repeatedly pointed out, however that these results, either measured or calculated should be regarded as rough estimates providing useful additional information rather than exact thicknesses of surface layers transformed during the accelerated *in vitro* ageing.

The results of preliminary mechanical testing performed on four specimens from each group that were aged for 24 h are presented in Fig. 10. The preponderate reason that made us include these preliminary results into the present work was that the lowest bi-axial flexural strength value obtained from the total of 32 specimens was 955 MPa, the and second lowest being 980 MPa, all remaining 30 specimens failed at a fracture stress level higher than 1 GPa. These values are considerably higher than commonly reported mean bi-axial strength values obtained with pressure-less sintered TZ-3YSB-E ceramics (typically ranging

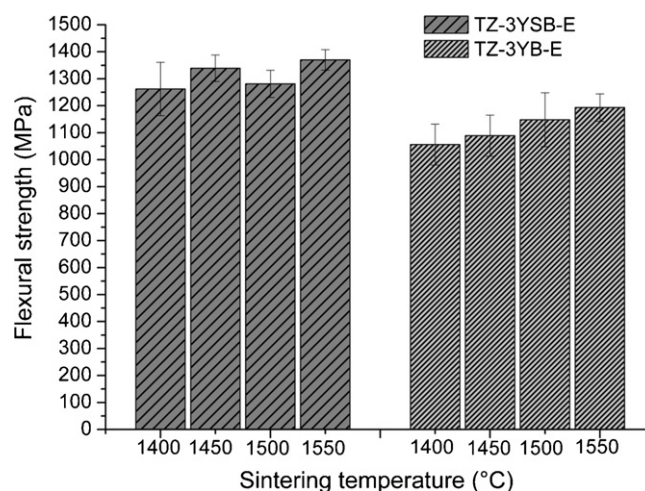


Fig. 10. Bi-axial flexural strength of the TZ-3YB-E and TZ-3YSB-E ceramics *versus* sintering temperature after the specimens were subjected to *in vitro* ageing for 24 h at 134 °C.

from about 900–1150 MPa)^{18,28–32} and are similar to the bi-axial flexural strength of sandblasted TZ-3YSB-E ceramics also exhibiting surface strengthening³³. Being so, we are pretty confident in saying that after 24 h of accelerated *in vitro* ageing none of the tested 32 specimens was seriously degraded.

4. Conclusions

From the present *in vitro* study designed to monitor the t–m transformation of bio-medical grade 3Y-TZP ceramics produced from two ready-to-press granulated powders of the same nominal chemical composition, but differing in their specific surface area, the following conclusions can be drawn:

- (i) the starting powder characteristics (in particular the BET) strongly influences the initial stages of sintering, during which the surface diffusion is prevailing, whereas during the last stage of sintering, which is dominated by the volume diffusion and grain-boundary mobility, the effect of the starting powder characteristics becomes almost negligible.
- (ii) increasing the sintering temperature will result in coarser microstructures of the specimens. Irrespective of the difference in the specific surface area of the starting TZ-3YB-E and TZ-3YSB-E powders, the ceramic microstructures after sintering under the same conditions were practically identical, being unimodal, exhibiting similar grain sizes and with practically no pore inclusions. The amount of the monoclinic (m-ZrO₂) and the rhombohedral (cubic 2; r-ZrO₂) fractions in all the sintered specimens was below the detection limit.
- (iii) After accelerated *in vitro* ageing, the peaks of the monoclinic, tetragonal, cubic and rhombohedral zirconia were observed; their relative fractions varied depending on the starting powder, sintering temperature and ageing time.
- (iv) Materials sintered at higher temperatures initially transform at a higher rate than those sintered at lower temperatures. There was a marked difference in ageing behavior between the two materials sintered at the lowest sintering temperature of 1400 °C indicating that in this case the grain size was not the prevailing factor influencing the transformability of the tetragonal zirconia (t-ZrO₂) under hydrothermal conditions.
- (v) Two alternative methods were used in order to estimate the thickness of the transformed surface layers. In spite of several uncertainties and inherent limitations pertaining to the XRD and SEM determination methods, the agreement of the results was quite remarkable.
- (vi) The results of the preliminary mechanical testing did not reveal any noticeable strength degradation after 24 h of accelerated *in vitro* ageing.

Acknowledgment

The support by the Ministry of Higher Education, Science and Technology of the Republic of Slovenia within the National Research Program is gratefully acknowledged.

References

1. Kelly JR. Ceramics in restorative and prosthetic dentistry. *Annu Rev Mater Sci* 1997;**27**:443–68.
2. Kappert HF. Dental materials: new ceramic systems. *Trans Acad Dent Mater* 1996;**9**:180–99.
3. Denry I, Kelly JR. State of the art of zirconia for dental applications. *Dent Mater* 2008;**24**:299–307.
4. Hondrum SO. A review of strength properties of dental ceramics. *J Prosthet Dent* 1992;**67**:859–65.
5. Tinschert J, Zwez D, Marx R, Anusavice KJ. Structural reliability of alumina-, feldspar-, leucite-, mica- and zirconia-based ceramics. *J Dent* 2000;**28**:529–35.
6. Guazzato M, Albakry M, Ringer SP, Swain MV. Strength, fracture toughness and microstructure of a selection of all-ceramic materials. Part II. Zirconia-based dental ceramics. *Dent Mater* 2004;**20**:449–56.
7. Kelly JR, Denry I. Stabilized zirconia as a structural ceramic: an overview. *Dent Mater* 2008;**24**:289–98.
8. Raigrodski AJ. All-ceramic full-coverage restorations: concepts and guidelines for material selection. *Pract Periodontics Aesthet Dent* 2008;**17**:249–56.
9. Hidaka O, Iwasaki M, Saito M, Morimoto T. Influence of clenching intensity on bite force balance, occlusal contact area, and average bite pressure. *J Dent Res* 1999;**78**:1336–44.
10. Addison O, Fleming GJ, Marquis PM. The effect of thermocycling on the strength of porcelain laminate veneer materials. *Dent Mater* 2003;**19**:291–7.
11. Kobayashi K, Kuwajima H, Masaki T. Phase change and mechanical properties of ZrO₂Y₂O₃ solid electrolyte after ageing. *Solid State Ionics* 1981;**3/4**:489–93.
12. Lawson S. Environmental degradation of zirconia ceramics. *J Eur Ceram Soc* 1995;**15**:485–502.
13. Chevalier J. What future for zirconia as a biomaterial? *Biomaterials* 2006;**27**:535–43.
14. Jevnikar P, Serša I, Sepe A, Jarh O, Funduk N. Effect of surface coating on water migration into resin-modified glass ionomer cements: a magnetic resonance micro-imaging study. *Magn Reson Med* 2000;**44**:686–91.
15. Garvie RC, Nicholson PS. Phase analysis in zirconia systems. *J Am Ceram Soc* 1972;**55**:303–5.
16. Kosmač T, Wagner R, Claussen N. X-ray determination of transformation depths in ceramics containing tetragonal ZrO₂. *J Am Ceram Soc* 1981;**64**:C72–3.
17. Gupta TK, Bechtold JH, Kuznicki RC, Cadoff LH, Rossing BR. Stabilization of tetragonal phase in polycrystalline zirconia. *J Mater Sci* 1977;**12**:2421–6.
18. Ruiz L, Readey MJ. Effect of heat treatment on grain size, phase assemblage, and mechanical properties of 3 mol% Y-TZP. *J Am Ceram Soc* 1996;**79**:2331–40.
19. Scott HG. Phase relationships in the zirconia–yttria system. *J Mater Sci* 1975;**10**:1527–35.
20. Kitano Y, Mori Y, Ishitani A, Masaki T. A study of rhombohedral phase in Y₂O₃-partially stabilized zirconia. *Mater Res Soc Symp Proc* 1987;**78**:17–24.
21. Reed JS, Lejus AM. Affect of grinding and polishing on near surface transformation in zirconia. *Mater Res Bull* 1977;**12**:949–54.
22. Burke DP, Rainforth WM. Intermediate rhombohedral (r-ZrO₂) phase formation at the surface of sintered Y-TZP's. *J Mater Sci Lett* 1997;**16**:883–5.
23. Hasegawa H, Hioki T, Kamigaito O. Cubic-to-rhombohedral phase transformation in zirconia by ion implantation. *J Mater Sci Lett* 1985;**4**:1092–4.
24. Kim DJ, Jung HJ, Cho DH. Phase transformations of Y₂O₃ and Nb₂O₅ doped tetragonal zirconia during low temperature aging in air. *Solid State Ionics* 1995;**80**:67–73.
25. Andrzejczuk M, Lewandowska M, Kosmač T, Kurzydowski KJ. Hydrothermal degradation of zirconia ceramics. *Adv Mater Sci* 2007;**7**:76–85.
26. Deville S, Chevalier J. Martensitic relief observation by atomic force microscopy in yttria-stabilized zirconia. *J Am Ceram Soc* 2003;**86**:2225–7.

27. Munoz-Tabares JA, Jimenez-Pique E, Anglada M. Subsurface evaluation of hydrothermal degradation of zirconia. *Acta Mater* 2011;**59**:473–84.
28. Kosmač T, Oblak Č, Jevnikar P, Funduk N, Marion L. Strength and reliability of surface treated Y-TZP dental ceramics. *J Biomed Mater Res* 2000;**53**:304–13.
29. Papanagiotou HP, Morgano SM, Giordano RA, Pober R. In vitro evaluation of low-temperature aging effects and finishing procedures on the flexural strength and structural stability of Y-TZP dental ceramics. *J Prosthet Dent* 2006;**96**:154–64.
30. Pittayachawan P, McDonald A, Young A, Knowles JC. Flexural strength, fatigue life, and stress-induced phase transformation study of Y-TZP dental ceramic. *J Biomed Mater Res B Appl Biomater* 2009;**88B**:366–77.
31. Pittayachawan P, McDonald A, Petrie A, Knowles JC. The biaxial flexural strength and fatigue property of Lava™ Y-TZP dental ceramic. *Dent Mater* 2007;**23**:1018–29.
32. Munoz-Tabares JA, Jimenez-Pique E, Reyes-Gasga J, Anglada M. Microstructural changes in ground 3Y-TZP and their effect on mechanical properties. *Acta Mater* 2011;**59**:6670–83.
33. Kosmač T, Oblak Č, Marion L. The effects of dental grinding and sandblasting on ageing and fatigue behavior of dental zirconia (Y-TZP) ceramics. *J Eur Ceram Soc* 2008;**28**:1085–90.